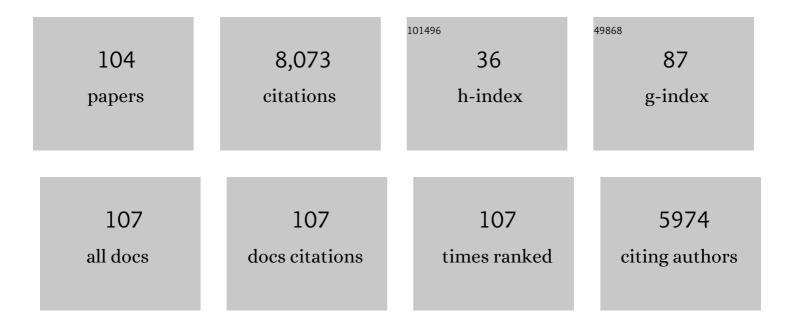
Marc Delarue

List of Publications by Year in descending order

Source: https://exaly.com/author-pdf/7527248/publications.pdf Version: 2024-02-01



#	Article	IF	CITATIONS
1	How cyanophage S-2L rejects adenine and incorporates 2-aminoadenine to saturate hydrogen bonding in its DNA. Nature Communications, 2021, 12, 2420.	5.8	24
2	Fast and efficient purification of SARS-CoV-2 RNA dependent RNA polymerase complex expressed in Escherichia coli. PLoS ONE, 2021, 16, e0250610.	1.1	5
3	Simultaneous Identification of Multiple Binding Sites in Proteins: A Statistical Mechanics Approach. Journal of Physical Chemistry B, 2021, 125, 5052-5067.	1.2	1
4	Parameterizing elastic network models to capture the dynamics of proteins. Journal of Computational Chemistry, 2021, 42, 1643-1661.	1.5	11
5	Characterization of a triad of genes in cyanophage S-2L sufficient to replace adenine by 2-aminoadenine in bacterial DNA. Nature Communications, 2021, 12, 4710.	5.8	15
6	Physics approach to the variable-mass optimal-transport problem. Physical Review E, 2021, 103, 012113.	0.8	6
7	Structural dynamics and determinants of 2-aminoadenine specificity in DNA polymerase DpoZ of vibriophage I•VC8. Nucleic Acids Research, 2021, 49, 11974-11985.	6.5	5
8	Extracting Dynamical Correlations and Identifying Key Residues for Allosteric Communication in Proteins by <i>correlationplus</i> . Journal of Chemical Information and Modeling, 2021, 61, 4832-4838.	2.5	21
9	Structural Studies of HNA Substrate Specificity in Mutants of an Archaeal DNA Polymerase Obtained by Directed Evolution. Biomolecules, 2020, 10, 1647.	1.8	7
10	Structural basis for allosteric transitions of a multidomain pentameric ligand-gated ion channel. Proceedings of the National Academy of Sciences of the United States of America, 2020, 117, 13437-13446.	3.3	18
11	Structural basis for the increased processivity of D-family DNA polymerases in complex with PCNA. Nature Communications, 2020, 11, 1591.	5.8	34
12	Structural evidence for the binding of monocarboxylates and dicarboxylates at pharmacologically relevant extracellular sites of a pentameric ligand-gated ion channel. Acta Crystallographica Section D: Structural Biology, 2020, 76, 668-675.	1.1	6
13	Statistical Physics Approach to the Optimal Transport Problem. Physical Review Letters, 2019, 123, 040603.	2.9	11
14	Optimal transport at finite temperature. Physical Review E, 2019, 100, 013310.	0.8	8
15	Structural evidence for an in trans base selection mechanism involving Loop1 in polymerase μ at an NHEJ double-strand break junction. Journal of Biological Chemistry, 2019, 294, 10579-10595.	1.6	7
16	Structure of the DP1–DP2 PolD complex bound with DNA and its implications for the evolutionary history of DNA and RNA polymerases. PLoS Biology, 2019, 17, e3000122.	2.6	30
17	Rapid enzymatic synthesis of long RNA polymers: A simple protocol to generate RNA libraries with random sequences. Methods, 2019, 161, 83-90.	1.9	1
18	Numerical Encodings of Amino Acids in Multivariate Gaussian Modeling of Protein Multiple Sequence Alignments. Molecules, 2019, 24, 104.	1.7	2

Marc Delarue

#	Article	IF	CITATIONS
19	An updated structural classification of replicative DNA polymerases. Biochemical Society Transactions, 2019, 47, 239-249.	1.6	34
20	Coarse-grained dynamics of supramolecules: Conformational changes in outer shells of Dengue viruses. Progress in Biophysics and Molecular Biology, 2019, 143, 20-37.	1.4	3
21	Terminal deoxynucleotidyltransferase: the story of an untemplated DNA polymerase capable of DNA bridging and templated synthesis across strands. Current Opinion in Structural Biology, 2018, 53, 22-31.	2.6	27
22	Crystal structures of a pentameric ion channel gated by alkaline pH show a widely open pore and identify a cavity for modulation. Proceedings of the National Academy of Sciences of the United States of America, 2018, 115, E3959-E3968.	3.3	26
23	Structural Basis for a Bimodal Allosteric Mechanism of General Anesthetic Modulation in Pentameric Ligand-Gated Ion Channels. Cell Reports, 2018, 23, 993-1004.	2.9	33
24	Electrostatics, proton sensor, and networks governing the gating transition in GLIC, a proton-gated pentameric ion channel. Proceedings of the National Academy of Sciences of the United States of America, 2018, 115, E12172-E12181.	3.3	30
25	Enzymatic synthesis of random sequences of RNA and RNA analogues by DNA polymerase theta mutants for the generation of aptamer libraries. Nucleic Acids Research, 2018, 46, 6271-6284.	6.5	16
26	Combined approaches from physics, statistics, and computer science for ab initio protein structure prediction: ex unitate vires (unity is strength)?. F1000Research, 2018, 7, 1125.	0.8	9
27	Secret From the ABYSS: Structures of the D-Family DNA Polymerase (POLD) Reveal that DNA Replication and DNA Transcription Share a Joint Evolutionary History in Archaea. Biophysical Journal, 2018, 114, 218a.	0.2	0
28	Meet-U: Educating through research immersion. PLoS Computational Biology, 2018, 14, e1005992.	1.5	4
29	The Renormalization Group and Its Applications to Generating Coarse-Grained Models of Large Biological Molecular Systems. Journal of Chemical Theory and Computation, 2017, 13, 1424-1438.	2.3	16
30	String method solution of the gating pathways for a pentameric ligand-gated ion channel. Proceedings of the National Academy of Sciences of the United States of America, 2017, 114, E4158-E4167.	3.3	60
31	Barbiturates Bind in the GLIC Ion Channel Pore and Cause Inhibition by Stabilizing a Shut State. Biophysical Journal, 2017, 112, 553a.	0.2	Ο
32	Barbiturates Bind in the GLIC Ion Channel Pore and Cause Inhibition by Stabilizing a Closed State. Journal of Biological Chemistry, 2017, 292, 1550-1558.	1.6	19
33	<i>Ab initio</i> sampling of transition paths by conditioned Langevin dynamics. Journal of Chemical Physics, 2017, 147, 152703.	1.2	22
34	Full mutational mapping of titratable residues helps to identify proton-sensors involved in the control of channel gating in the Gloeobacter violaceus pentameric ligand-gated ion channel. PLoS Biology, 2017, 15, e2004470.	2.6	24
35	Identification of a pre-active conformation of a pentameric channel receptor. ELife, 2017, 6, .	2.8	36
36	Comparative Normal Mode Analysis of the Dynamics of DENV and ZIKV Capsids. Frontiers in Molecular Biosciences, 2016, 3, 85.	1.6	11

#	Article	IF	CITATIONS
37	Sites of Anesthetic Inhibitory Action on a Cationic Ligand-Gated Ion Channel. Structure, 2016, 24, 595-605.	1.6	35
38	Beyond Poisson–Boltzmann: Numerical Sampling of Charge Density Fluctuations. Journal of Physical Chemistry B, 2016, 120, 6270-6277.	1.2	3
39	Structural Basis for a New Templated Activity by Terminal Deoxynucleotidyl Transferase: Implications for V(D)J Recombination. Structure, 2016, 24, 1452-1463.	1.6	28
40	Shared active site architecture between archaeal PolD and multi-subunit RNA polymerases revealed by X-ray crystallography. Nature Communications, 2016, 7, 12227.	5.8	40
41	Structural Basis for Xenon Inhibition in a Cationic Pentameric Ligand-Gated Ion Channel. PLoS ONE, 2016, 11, e0149795.	1.1	31
42	Allosteric and hyperekplexic mutant phenotypes investigated on an α ₁ glycine receptor transmembrane structure. Proceedings of the National Academy of Sciences of the United States of America, 2015, 112, 2865-2870.	3.3	56
43	Genuine open form of the pentameric ligand-gated ion channel GLIC. Acta Crystallographica Section D: Biological Crystallography, 2015, 71, 454-460.	2.5	25
44	Structural basis for a novel mechanism of <scp>DNA</scp> bridging and alignment in eukaryotic <scp>DSB DNA</scp> repair. EMBO Journal, 2015, 34, 1126-1142.	3.5	21
45	Crystallographic studies of pharmacological sites in pentameric ligand-gated ion channels. Biochimica Et Biophysica Acta - General Subjects, 2015, 1850, 511-523.	1.1	46
46	Modified Poisson–Boltzmann equations for characterizing biomolecular solvation. Journal of Theoretical and Computational Chemistry, 2014, 13, 1440001.	1.8	13
47	Enhanced Amino Acid Selection in Fully Evolved Tryptophanyl-tRNA Synthetase, Relative to Its Urzyme, Requires Domain Motion Sensed by the D1 Switch, a Remote Dynamic Packing Motif. Journal of Biological Chemistry, 2014, 289, 4367-4376.	1.6	33
48	Crystal structures of a pentameric ligand-gated ion channel provide a mechanism for activation. Proceedings of the National Academy of Sciences of the United States of America, 2014, 111, 966-971.	3.3	175
49	Structural Basis for Allosteric Transitions in the GLIC Pentameric Proton-Gated Ion Channel. Biophysical Journal, 2014, 106, 343a.	0.2	0
50	New Nucleotide-Competitive Non-Nucleoside Inhibitors of Terminal Deoxynucleotidyl Transferase: Discovery, Characterization, and Crystal Structure in Complex with the Target. Journal of Medicinal Chemistry, 2013, 56, 7431-7441.	2.9	24
51	Structural basis for ion permeation mechanism in pentameric ligand-gated ion channels. EMBO Journal, 2013, 32, 728-741.	3.5	140
52	Structures of Intermediates along the Catalytic Cycle of Terminal Deoxynucleotidyltransferase: Dynamical Aspects of the Two-Metal Ion Mechanism. Journal of Molecular Biology, 2013, 425, 4334-4352.	2.0	41
53	Computational Assembly of Polymorphic Amyloid Fibrils Reveals Stable Aggregates. Biophysical Journal, 2013, 104, 683-693.	0.2	36
54	Structural basis for potentiation by alcohols and anaesthetics in a ligand-gated ion channel. Nature Communications, 2013, 4, 1697.	5.8	126

#	Article	IF	CITATIONS
55	2′â€Đeoxyribonucleoside Phosphoramidate Triphosphate Analogues as Alternative Substrates for <i>E. coli</i> Polymerase III. ChemBioChem, 2012, 13, 2439-2444.	1.3	9
56	Molecular Recognition of Canonical and Deaminated Bases by P. abyssi Family B DNA Polymerase. Journal of Molecular Biology, 2012, 423, 315-336.	2.0	36
57	A locally closed conformation of a bacterial pentameric proton-gated ion channel. Nature Structural and Molecular Biology, 2012, 19, 642-649.	3.6	135
58	Structure and Pharmacology of Pentameric Receptor Channels: From Bacteria to Brain. Structure, 2012, 20, 941-956.	1.6	202
59	X-ray structures of general anaesthetics bound to a pentameric ligand-gated ion channel. Nature, 2011, 469, 428-431.	13.7	407
60	AquaSAXS: a web server for computation and fitting of SAXS profiles with non-uniformally hydrated atomic models. Nucleic Acids Research, 2011, 39, W184-W189.	6.5	91
61	Atomic structure and dynamics of pentameric ligand-gated ion channels: new insight from bacterial homologues. Journal of Physiology, 2010, 588, 565-572.	1.3	102
62	One-microsecond molecular dynamics simulation of channel gating in a nicotinic receptor homologue. Proceedings of the National Academy of Sciences of the United States of America, 2010, 107, 6275-6280.	3.3	159
63	Crystal Structure of the Extracellular Domain of a Bacterial Ligand-Gated Ion Channel. Journal of Molecular Biology, 2010, 395, 1114-1127.	2.0	52
64	Structural Insights into the Quinolone Resistance Mechanism of Mycobacterium tuberculosis DNA Gyrase. PLoS ONE, 2010, 5, e12245.	1.1	118
65	Structure of the Archaeal Pab87 Peptidase Reveals a Novel Self-Compartmentalizing Protease Family. PLoS ONE, 2009, 4, e4712.	1.1	23
66	Independent saturation of three TrpRS subsites generates a partially assembled state similar to those observed in molecular simulations. Proceedings of the National Academy of Sciences of the United States of America, 2009, 106, 1790-1795.	3.3	28
67	Conferring a template-dependent polymerase activity to terminal deoxynucleotidyltransferase by mutations in the Loop1 region. Nucleic Acids Research, 2009, 37, 4642-4656.	6.5	28
68	X-ray structure of a pentameric ligand-gated ion channel in an apparently open conformation. Nature, 2009, 457, 111-114.	13.7	644
69	Computing Ion Solvation Free Energies Using the Dipolar Poisson Model. Journal of Physical Chemistry B, 2009, 113, 5694-5697.	1.2	25
70	Insights Into the Enzymatic Mechanism of 6-Phosphogluconolactonase from Trypanosoma brucei Using Structural Data and Molecular Dynamics Simulation. Journal of Molecular Biology, 2009, 388, 1009-1021.	2.0	16
71	Dealing with structural variability in molecular replacement and crystallographic refinement through normal-mode analysis. Acta Crystallographica Section D: Biological Crystallography, 2008, 64, 40-48.	2.5	20
72	Incorporating Dipolar Solvents with Variable Density in Poisson-Boltzmann Electrostatics. Biophysical Journal, 2008, 95, 5587-5605.	0.2	73

#	Article	IF	CITATIONS
73	MinActionPath: maximum likelihood trajectory for large-scale structural transitions in a coarse-grained locally harmonic energy landscape. Nucleic Acids Research, 2007, 35, W477-W482.	6.5	76
74	Three Dimensional Structure and Implications for the Catalytic Mechanism of 6-Phosphogluconolactonase from Trypanosoma brucei. Journal of Molecular Biology, 2007, 366, 868-881.	2.0	21
75	Determination of dihedral Î [.] angles in large proteins by combining NHN/CαHα dipole/dipole cross-correlation and chemical shifts. Proteins: Structure, Function and Bioinformatics, 2006, 64, 931-939.	1.5	4
76	PDB_Hydro: incorporating dipolar solvents with variable density in the Poisson-Boltzmann treatment of macromolecule electrostatics. Nucleic Acids Research, 2006, 34, W38-W42.	6.5	62
77	NOMAD-Ref: visualization, deformation and refinement of macromolecular structures based on all-atom normal mode analysis. Nucleic Acids Research, 2006, 34, W52-W56.	6.5	292
78	An asymmetric underlying rule in the assignment of codons: Possible clue to a quick early evolution of the genetic code via successive binary choices. Rna, 2006, 13, 161-169.	1.6	47
79	Refinement of docked protein-ligand and protein-DNA structures using low frequency normal mode amplitude optimization. Nucleic Acids Research, 2005, 33, 4496-4506.	6.5	62
80	Normal Mode Analysis Suggests a Quaternary Twist Model for the Nicotinic Receptor Gating Mechanism. Biophysical Journal, 2005, 88, 3954-3965.	0.2	178
81	On the use of low-frequency normal modes to enforce collective movements in refining macromolecular structural models. Proceedings of the National Academy of Sciences of the United States of America, 2004, 101, 6957-6962.	3.3	187
82	Enzymatic and Structural Analysis of Inhibitors Designed against Mycobacterium tuberculosis Thymidylate Kinase. Journal of Biological Chemistry, 2003, 278, 4963-4971.	1.6	82
83	Simplified Normal Mode Analysis of Conformational Transitions in DNA-dependent Polymerases: the Elastic Network Model. Journal of Molecular Biology, 2002, 320, 1011-1024.	2.0	243
84	Cryophotolysis of caged compounds: a technique for trapping intermediate states in protein crystals. Acta Crystallographica Section D: Biological Crystallography, 2002, 58, 607-614.	2.5	34
85	Crystal structures of a template-independent DNA polymerase: murine terminal deoxynucleotidyltransferase. EMBO Journal, 2002, 21, 427-439.	3.5	138
86	Resolution of the phase-ambiguity problem in the centrosymmetric P ar{1} space group by Monte Carlo methods. Acta Crystallographica Section A: Foundations and Advances, 2000, 56, 554-561.	0.3	2
87	General formalism for phase combination and phase refinement: a statistical thermodynamics approach in reciprocal space. Acta Crystallographica Section A: Foundations and Advances, 2000, 56, 562-574.	0.3	5
88	Aspartyl tRNA-synthetase from Escherichia coli: flexibility and adaptability to the substrates. Journal of Molecular Biology, 2000, 299, 1157-1164.	2.0	36
89	Solution structural studies and low-resolution model of the Schizosaccharomyces pombe sap1 protein. Journal of Molecular Biology, 2000, 300, 563-574.	2.0	40
90	Building protein lattice models using self-consistent mean field theory. Journal of Chemical Physics, 1998, 108, 9540-9549.	1.2	14

#	Article	IF	CITATIONS
91	Cloning and characterisation of a gene from Plasmodium vivax and P. knowlesi: homology with valine-tRNA synthetase. Gene, 1996, 173, 137-145.	1.0	2
92	Mean-field minimization methods for biological macromolecules. Current Opinion in Structural Biology, 1996, 6, 222-226.	2.6	77
93	[40] Converting sequence block alignments into structural insights. Methods in Enzymology, 1996, 266, 662-680.	0.4	4
94	Partition of aminoacyl-tRNA synthetases in two different structural classes dating back to early metabolism: Implications for the origin of the genetic code and the nature of protein sequences. Journal of Molecular Evolution, 1995, 41, 703-11.	0.8	15
95	Structure of phenylalanyl-tRNA synthetase from Thermus thermophilus. Nature Structural Biology, 1995, 2, 537-547.	9.7	145
96	Atomic Environment Energies in Proteins Defined from Statistics of Accessible and Contact Surface Areas. Journal of Molecular Biology, 1995, 249, 675-690.	2.0	36
97	Polar and nonpolar atomic environments in the protein core: Implications for folding and binding. Proteins: Structure, Function and Bioinformatics, 1994, 20, 264-278.	1.5	86
98	Application of a Self-consistent Mean Field Theory to Predict Protein Side-chains Conformation and Estimate Their Conformational Entropy. Journal of Molecular Biology, 1994, 239, 249-275.	2.0	347
99	Crystallization and X-ray Crystallogragphic Analysis of Recombinant Chicken Poly (ADP-ribose) Polymerase Catalytic Domain Produced in Sf9 Insect Cells. Journal of Molecular Biology, 1994, 244, 114-116.	2.0	30
100	Synthesis and Recognition of Aspartyl-adenylate by Thermus thermophilus Aspartyl-tRNA Synthetase. Journal of Molecular Biology, 1994, 244, 158-167.	2.0	73
101	Crystal Structure of Cleaved Bovine Antithrombin III at 3·2 à Resolution. Journal of Molecular Biology, 1993, 232, 223-241.	2.0	110
102	Three-dimensional structure of phenylalanyl-transfer RNA synthetase from Thermus thermophilus HB8 at 0.6-nm resolution. FEBS Journal, 1992, 208, 411-417.	0.2	9
103	Partition of tRNA synthetases into two classes based on mutually exclusive sets of sequence motifs. Nature, 1990, 347, 203-206.	13.7	1,372
104	An attempt to unify the structure of polymerases. Protein Engineering, Design and Selection, 1990, 3, 461-467.	1.0	616